Applied Surface Science xxx (2014) xxx–xxx

Contents lists available at ScienceDirect

Applied Surface Science

journal homepage: www.elsevier.com/locate/apsusc

CO adsorption on PdGa(1 0 0), (1 1 1) and ($\bar{1}\,\bar{1}\,\bar{1}$) surfaces: A DFT study

P. Bechthold, J.S. Ardhengi, A. Juan*, E.A. González, P.V. Jasen

Departamento de Física & IFISUR (UNS-CONICET) - Universidad Nacional del Sur Av. Alem 1253, 8000 Bahía Blanca, Argentina

ARTICLE INFO

Article history:
Received 29 October 2013
Received in revised form 11 January 2014
Accepted 13 January 2014
Available online xxx

Keywords:
PdGa
DFT
Intermetallic compounds
CO adsorption

ABSTRACT

CO adsorption on (1 0 0), (1 1 1) and ($\bar{1}\,\bar{1}\,\bar{1}$) planes is analyzed using density functional theory (DFT) calculations. Changes in the electronic structure of these surfaces and CO bond after adsorption are also addressed here. CO is located on Pd atop geometry with a tilted configuration of 7.8° in the (1 0 0) plane, while in the (1 1 1) and ($\bar{1}\,\bar{1}\,\bar{1}$) are perpendicular to the surface. No direct interaction of CO with Ga is detected. The overlap population (OP) of Pd-Pd and Pd-Ga bond decreases as the new Pd-CO bond is formed. In all cases, the C-O bond length changes less than 1% compared to the vacuum but its strength decrease about 50% as determined by the changes in the OP. The effect of CO is limited to its first Pd neighbor. Analysis of orbital interaction reveals that Pd-CO bond mainly involves s-s and s-p orbitals with less participation of Pd 4d orbitals. Computed CO vibration frequencies after adsorption shows a red shift from vacuum towards 1972.9, 1990.4 and 1988.6 cm^{-1} on (1 0 0), (1 1 1) and ($\bar{1}\,\bar{1}\,\bar{1}$) planes respectively, following the same trend that experimental data on the PdGa intermetallic compound.

1. Introduction

The PdGa intermetallic compound (IMC) is an interesting bimetallic system that has been beginning studied in the recent years both from a theoretical and an experimental point of view. The intermetallic compound concept is basically a chemical compound of two or more metallic elements that adopts an at least partly ordered crystal structure that differs from those of the constituent metals. Intermetallic compounds are single-phase materials and often hold a wide homogeneity range [1]. The principal idea behind the intermetallic compound concept is to obtain long-term stable catalysts with preselected electronic and local structural properties.

Energy carriers are used to store, move and deliver energy in an easily usable form. The conversion of energy to electricity makes easy its transportation. Hydrogen is one of the most promising energy carriers for the future. It is a high efficiency, low polluting fuel that can be used for transportation, heating, and power generation in places where it is difficult to use electricity [2]. Since hydrogen gas is not found free on Earth, it must be manufactured. There are four basic methods for hydrogen production at present: steam reforming reaction, partial oxidation, auto-thermal reforming and water electrolysis.

Methanol steam reforming (MSR, $CH_3OH + H_2O \rightarrow 3H_2 + CO_2$) is considered as one of the most promising ways to produce high purity hydrogen for mobile fuel cell applications. However, the main drawback is the formation of CO as a byproduct, which has to be kept at a level of less than 20 ppm to prevent poisoning of fuel cell electrodes.

Several Pd-based catalysts have been studied [3–8] in search of possible alternatives to be used in efficient hydrogen production. However, this system are far from single-phase materials and its difficult to rationalize experimental results.

Recently, Rameshan et al. [9] made a XPS study of methanol reforming on a PdGa near-surface intermetallic phase (NSIP). There is a difference between IMC and NSIP the first is thermodynamically stable, the second one is not. In addition, the crystal structure of the NSIP is unknown. The authors report that this NSIP is a poor unselective catalyst in MSR, but it is highly CO_2 selective and active in the presence of O_2. Therefore, this unsupported catalyst could be used in an oxidative methanol steam reforming process (OMSR, $CH_3OH + 1/2O_2 \rightarrow 2H_2 + CO_2$) in order to obtain hydrogen. The advantage of using an unsupported catalyst, instead of the supported catalyst commonly used, is that the composition of the catalyst surface is well defined and it presents more structural stability and less deactivation.

Krajčí and Hafner investigated the {1 1 1} threefold surfaces polar character of the GaPd compound using density-functional methods [10]. Because of the lack of inversion symmetry, the B20 structure exists in two enantiomorphic forms denoted as A and B, as in [11,12]. In both non-equivalent (1 1 1) and ($\bar{1}\,\bar{1}\,\bar{1}$) directions, the

* Corresponding author. Tel.: +54 291 4595101 Ext: 2818; fax: +54 0291 4595142.
E-mail address: cajuan@uns.edu.ar (A. Juan).

http://dx.doi.org/10.1016/j.apsusc.2014.01.074
0169-4332/

formation of several surfaces differing in structure and chemical composition is possible. Eight possible surface terminations with different atomic layers in surface and sub-surface positions were identified. The surface energies calculated are in agreement with a simulated cleavage experiment. However, cleavage does not result in the formation of the lowest-energy surfaces, because all possible {1 1 1}-cleavage planes expose a low-energy surface on one side, and a high-energy surface on the other side. The calculated surface electronic density of states is in full agreement with photoemission spectroscopy experiments [10].

The concept of using intermetallic compounds with covalent bonding rather than alloys is a suitable way to arrive to long-term stable catalysts with pre-selected electronic and local structural properties [13–18].

The study of CO adsorption on Pd-Ga systems is rather scarce [2,9,10,13,19]. The purpose of the present work is to analyze CO adsorption on (1 0 0), (1 1 1) and ($\bar{1}\,\bar{1}\,\bar{1}$) surfaces of the PdGa intermetallic compound. This possible planes can be exposed at the real catalyst surface and the results can be compared with other plane – (1 1 0) – where we have performed DFT calculation [20,21]. With the aim of contributing to the understanding of the interactions between the CO – also an OMSR byproduct – and the intermetallic PdGa compound as catalyst, computational DFT calculations are performed to determine the binding energies of CO and the changes in the electronic structure and bonding in the intermetallic PdGa compound surfaces, after the CO adsorption.

2. Surface models and computational method

The PdGa intermetallic compound presents a $P2_13$ structure with a lattice parameter of $a_0 = 4.909$ Å [22–25]. The Bravais lattice is simple cubic, but the overall point symmetry is tetrahedral. In this structure, each atom has seven neighbors of the opposite chemical type (and vice-versa) and seven nearest neighboring bonds. In previous works we analyzed the effects of CO on PdGa (1 1 0) [21]. In order to continue with this study on the intermetallic compound, we have selected the low-index surfaces {1 0 0} and {1 1 1} for a better understanding of their adsorption capabilities. There are two reasons for selecting these surfaces: 1st this planes have higher stability than the (1 1 0) plane and 2nd to compare them with our previous calculations in the (1 1 0) plane. In the case of PdGa, the (1 0 0) surface is stoichometric and uniquely defined while the lack of inversion symmetry in the $P2_13$ structure makes the (1 1 1) and the ($\bar{1}\,\bar{1}\,\bar{1}$) surfaces non-equivalent. Density Functional Theory (DFT) is used to compute adsorption energies, trace relevant orbital interactions, and discuss the electronic consequences of incorporating CO to the surfaces. In the next sections we will consider the computational method and adsorption models.

2.1. Computational method

We performed first-principles calculations based on spin polarized DFT. The Vienna *Ab-initio* Simulation Package (VASP) is used to solve Kohn-Sham equations with periodic boundary conditions and a plane wave basis set [26–28]. Electron-ion interactions were described by ultra-soft pseudopotentials [29], exchange and correlation energies were also calculated using the Revised Perdew-Burke-Ernzerhof form of the spin-polarized generalized gradient approximation (GGA-RPBE), which has been shown to give accurate values for adsorption energies of many molecular species [30]. We used a kinetic energy cutoff of 700 eV for all calculations. The self-consistency iteration was stopped when total energies are converged to within 10^{-6} eV. The Monkhorst-Pack scheme is used for k-point sampling [31]. An equilibrium lattice constant of 4.899 Å is used as obtained with a $7 \times 7 \times 7$ converged mesh within the first Brillouin Zone. Geometry optimization was terminated when the Hellman-Feyman force on each atom was less than 0.05 eV/Å. The lattice constant is in agreement with experimental XRD data. Bader analysis is used to calculate electronic charges on atoms before and after CO adsorption [32]. The adsorption energy is calculated using the following equation:

$$\Delta E_{ads} = E_{Total}(CO/PdGa) - E_{Total}(PdGa) - E_{Total}(CO) \quad (1)$$

Here the first term on the right-hand side is the total energy of the super cell that includes 32 Pd and 32 Ga atoms in the plane (1 0 0), or 84 Pd and 84 Ga atoms for (1 1 1) and ($\bar{1}\,\bar{1}\,\bar{1}$) plus one CO molecule. The second term is the total energy of the intermetallic super-cell; the third term is the CO molecule total energy. The last one is calculated by placing CO in a cubic box with 10 Å sides and carrying out a Γ-point calculation. We obtained a CO bond length of 1.143 Å in good agreement with experimental values (1.131 Å) [33].

In order to understand CO-PdGa interactions and bonding we used the concept of Density of States (DOS) and the Crystal Orbital Overlap Population (COOP) as described by Hoffmann [34]. The COOP curve is a plot of the OP weighted DOS vs. energy. Looking at the COOP, we analyzed the extent to which specific states contribute to a bond between atoms or orbitals [34]. The SIESTA code is used to compute COOPs [35,36].

2.2. Surfaces and adsorption model

The (1 0 0), (1 1 1) and ($\bar{1}\,\bar{1}\,\bar{1}$) planes are represented with a super-cell. In order to achieve the best compromise between computational time and accuracy for our model, we decided to use a seven-layer slab separated in the corresponding perpendicular-direction by vacuum regions. The thickness of the vacuum region, corresponding to 14 Å, was enough in order to avoid the interaction with the images. It should be pointed out that each "layer" of slab is formed by two "sub-layers", presenting atoms above and below for the (1 0 0) surface (see Fig. 1a); and four "sub-layers" for the (1 1 1) and ($\bar{1}\,\bar{1}\,\bar{1}$) surfaces (see Fig. 1b and c). We have also tested our calculations with slab of 9 and 11 layers – and the corresponding sub layers – and no further improvement in energy or noticeable differences in DOS were found. The thickness of the PdGa surfaces slab should be such that it approaches the electronic structure of 3D bulk PdGa in the innermost layer. The (1 0 0) plane presents only one possible termination with a mixed composition while the (1 1 1) and ($\bar{1}\,\bar{1}\,\bar{1}$) planes presents several possible surface terminations, different in structure and chemical composition. In the last two cases, we analyzed only the Pd terminated surface because it presents better adsorption properties since Ga terminated surface usually does not adsorb CO. Recent calculations from our group corroborate this finding of non-active Ga as chemisorption sites for hydrogen and CO [20,21]. There are two possible Pd terminations, one that exposes Pd separated for more than 4.909 Å and the other one that exposes a Pd trimmer which correspond to PdGa:B(1 1 1) Pd_1 (PdGa:B ($\bar{1}\,\bar{1}\,\bar{1}$) Pd_1) - and PdGa:B (1 1 1) Pd_3 (PdGa:B ($\bar{1}\,\bar{1}\,\bar{1}$) Pd_3) according notation used by Rosenthal et al. [11]. We selected the first ones because we are interested in the so-called concept of Pd isolated sites.

In order to study of CO adsorption on the PdGa surfaces at low coverage, the CO-surface distance was optimized considering relaxation for the first four layers of the metal slab until 1 meV convergence was obtained in the total energy, maintaining the three remaining layers fixed (bulk like). Fig. 1 shows a schematic top (left) and side view (right) of the surfaces after CO adsorption.

Please cite this article in press as: P. Bechthold, et al., CO adsorption on PdGa(1 0 0), (1 1 1) and ($\bar{1}\,\bar{1}\,\bar{1}$) surfaces: A DFT study, Appl. Surf. Sci. (2014), http://dx.doi.org/10.1016/j.apsusc.2014.01.074

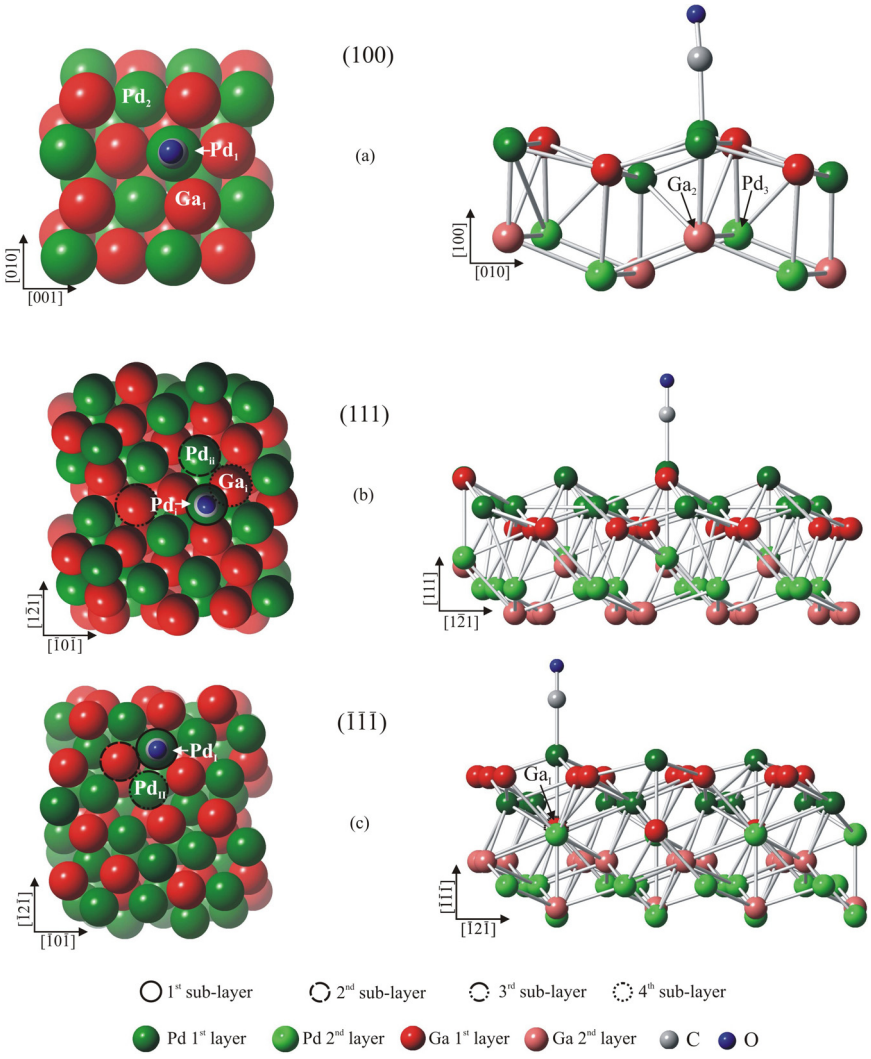

Fig. 1. Schematic top (right) and lateral (left) view of PdGa: (1 0 0) (a), (1 1 1) (b) and ($\bar{1}\bar{1}\bar{1}$) (c) surfaces after CO adsorption in the more stable geometry. For sake of clarity, only two first layers are shown.

3. Results and discussion

Considering the surface of the slab, the interlayer spacing in our models changes less than 1%, from the first to the inner layers, after geometry optimization. The distances between two adjacent Pd top sites on the surface are 4.908 Å, 6.827 Å and 6.921 Å in the (1 0 0), (1 1 1) and ($\bar{1}\,\bar{1}\,\bar{1}$) planes respectively and the mean Pd-Ga distances are 2.610 Å, 2.550 Å and 2.501 Å, respectively.

We have found different CO-adsorption geometries in the three surfaces considered. In all surfaces, the top Pd site is the most stable configuration at Pd-CO distances of 1.961, 1.976 and 1.958 Å (see Fig. 1) and adsorption energies of −1.41, −1.36 and −1.59 eV for PdGa (1 0 0), (1 1 1) and ($\bar{1}\,\bar{1}\,\bar{1}$) respectively (see Table 1). In the (1 1 1) and ($\bar{1}\,\bar{1}\,\bar{1}$) planes the CO adsorption is perpendicular to the surface, while in the (1 0 0) plane presents a 7.8° tilted configuration. In the (1 0 0) plane the bridge site is also stable but the top Ga site is not, thus supporting the idea that Ga terminations are not relevant for adsorption. For the (1 1 1) plane, the hollow site is not stable while in the ($\bar{1}\bar{1}\bar{1}$) plane it is stable but much less stable than the top site. Considering the CO adsorption on top site of a FCC Pd surface, Chen et al. reported −1.17 eV for the (1 1 1) plane while Pick found a corrected value of −1.19 eV in the (1 1 0) surface [37,38]. The last author also reports a Pd-CO distance of 1.91 Å. In the case of a Pd nano-clusters with a hybrid 5-fold-symmetry/close-packed structure, Paz-Borbon et al. obtained an adsorption energy of -1.42 eV for a CO bonded in a top position [39]. These results are full agreement with those reported by Krajčí and Hafner for the PdGa(1 1 1) and ($\bar{1}\,\bar{1}\,\bar{1}$) planes after CO adsorption [10]. The results for the ($\bar{1}\bar{1}\bar{1}$) plane can be compared with the thermal density spectroscopy (TDS) study by Rosenthal et al. [11]. The TDS spectrum shows a dominant peak at ≈210 K. This desorption peak was attributed to the CO bonded to the only one Pd atom/cell present in the surface layer. This assignment is compatible with our results. For a better understanding of this idea, we have calculated the minimal energy configuration for FCC Pd(1 1 1) which is in a hollow site with an adsorption energy of −2.35 eV. The differences between the energy values explain the higher desorption temperature (450 K) for the FCC Pd(1 1 1) surface (see Fig. 2).

We have also computed the stretching vibration frequencies for CO bonded to the surface. In order to do this, we used a whole vibrational mode that contributes to C-O bonding. The results are shown in Table 1. The experimental C-O frequency (gas phase) is 2170 cm^{-1} [40] while our computed values are close (2136.56 cm^{-1}) and this is in agreement with that reported by Lischka et al. [41]. Also the computed vibrational frequency values for the C-O bond are similar for all surfaces considered. The computed red shift of the CO vibrational frequencies is similar to that reported for the PdCO molecule and Pd_nCO clusters

Please cite this article in press as: P. Bechthold, et al., CO adsorption on PdGa(1 0 0), (1 1 1) and ($\bar{1}\,\bar{1}\,\bar{1}$) surfaces: A DFT study, Appl. Surf. Sci. (2014), http://dx.doi.org/10.1016/j.apsusc.2014.01.074

Table 1
Adsorption energies, vibrational frequencies, tilt angle, Pd-CO and C-O bond distances for the PdGa surfaces after CO adsorption.

	Surfaces						
	(1 0 0)			(1 1 1)		$(\bar{1}\,\bar{1}\,\bar{1})$	
	Top Pd[a]	Top Ga[a]	Bridge[a]	Top[a]	Hollow[a]	Top[a]	Hollow[a]
E_{ads} (eV/H)	−1.41	+0.67	−0.83	−1.36	+0.42	−1.59	−0.49
ν (cm^{-1})							
C-O	1972.9	–	–	1990.4	–	1988.6	–
Pd-CO	343.1			327.0		353.3	
Tilt angle (°)	7.8	–	–	0.1	–	0.1	–
Pd-CO (Å)	1.961	–	–	1.976	–	1.958	–
C-O (Å)	1.156	–	–	1.154	–	1.156	–

[a] Adsorption sites.

[42–47]. Föttinger observed a C-O frequency of 2047 cm^{-1}, on PdGa powder samples [48]. Our computed values fall in the range 1972.9–1990.4 cm^{-1}. We must emphasize that our models are build from clear cuts and a perfect IMC. The difference, with the case of PdGa supported samples, can be attributed to the limitations of our computational models that do not include any Pd or Ga vacancies, adatoms or impurities of any type. In the case of Pd-C frequencies, our results are within the range 234.30–256.60 cm^{-1} reported in [43].

Considering the electronic structure, the PdGa presents a significantly reduced electron density of the Fermi level with respect to the bulk (see Figs. 3–5). The Total DOS for the three surfaces considered looks similar. The Pd projected DOS for the (1 0 0) plane is similar to that already published for the plane (1 1 0) plane and shows a broad Pd 4d dominated band with a peak at about −2.9 eV. In the case of the (1 1 1) and $(\bar{1}\,\bar{1}\,\bar{1})$ plane, the Pd DOS projection is narrowed and two peaks are present, being the higher intensity peak shifted to the lower energies (see Figs. 3b, 4b and 5b, dashed red line). These results are in agreement with recent calculations made by Krajčí and Hafner [10]. In all cases, Ga projected DOS is represented by s- and p-like states (see Figs. 3c, 4c and 5c, dashed red line).

Regarding the bonding, the OP for Pd-Pd and Pd-Ga are presented in Table 2. The Pd-Pd OP in the (1 0 0) and (1 1 1) surfaces is about 0.106-0.118 at distances in the range of 3.007–3.011 Å for the bond between a superficial and an inner Pd atom. These values are higher than those obtained for Pd-Pd bulk (0.090). In the (1 0 0) plane, there is also an OP of 0.053 for the Pd-Pd superficial bond at a distance of 3.063 Å, which is lower than the bulk value. In the case of the $(\bar{1}\,\bar{1}\,\bar{1})$ surface, the Pd-Pd OP is close to the bulk value at a shorter bond distance (2.948 Å). Kovnir et al. using electron localization functions calculations (ELF/ELI) described the Pd-Pd interactions coming from three center bonds: Pd-Ga-Pd [1]. Similar type of bonding was also reported in the $CuAl_2$ IMC [49] ELF, COOP in combination with high-pressure X-ray diffraction and Raman spectroscopy show that this IMC has three-bonded aluminum atoms with the copper atoms inside the tetragonal-antiprismatic cavities. The Pd-Ga OP bond is higher than that of the bulk value in the (1 1 1) and $(\bar{1}\,\bar{1}\,\bar{1})$ surfaces (47.7% and 46.2%, respectively) at shorter distances (−8.2% and −9.6% compared to the bulk, respectively). However, in the (1 0 0) surface the Pd-Ga OP is lower than bulk values at distances of 2.607 and 2.643 Å.

Orbital by orbital contributions to the OP between atoms in the PdGa surfaces are summarized in Table 3. The main interactions are s-p, p-p and p-d followed by s-s. The s-s contribution is higher for the Pd-Pd bond in the (1 1 1) plane compared to the other surfaces. This is in line with a higher Pd s population. No d-d interaction is detected. Considering Pd-Ga bond, the s-p contribution is higher than 66% while a p-d contribution is close to 18%.

When CO is adsorbed, the C-O distance does not change significantly compared to the molecule in vacuum (see Table 2). Our computed C-O distance in vacuum is 1.143 Å, which is close to 1.131 Å determined from XRD data [33]. A similar C-O distance is also reported by Pick for CO/Pd(1 1 0) (1.168 Å) [38]. It should be mentioned that this author reports a perpendicular on-top geometry,

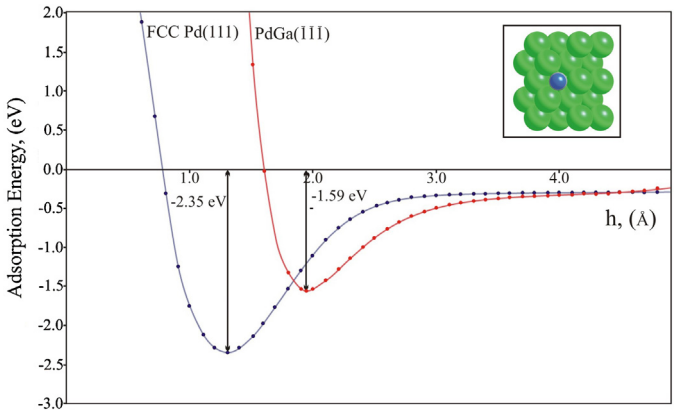

Fig. 2. Schematic for the adsorption energy (eV) vs. h (Å), where h is the perpendicular distances to surface for CO adsorbed in most stable site (top site in the case of PdGa and hollow for FCC elemental Pd). The insert is the schematic view of the Pd(1 1 1) after CO adsorption in the minimal configuration.

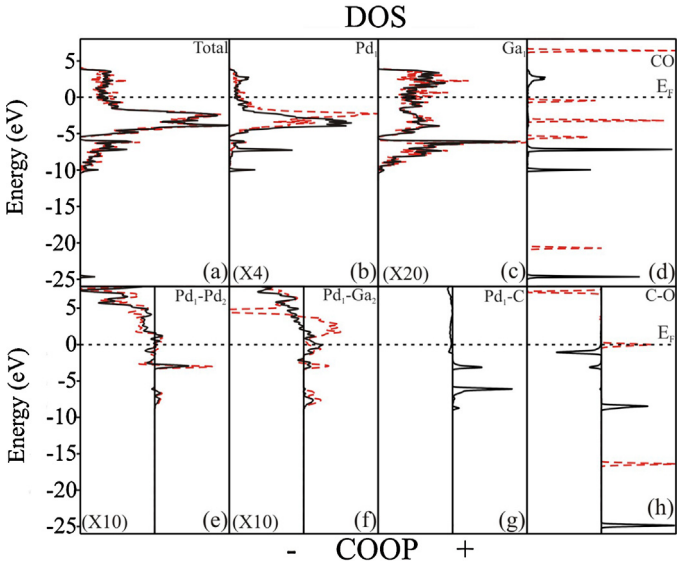

Fig. 3. Total DOS curves for the PdGa(1 0 0) surface (a); projected DOS for a Pd1 atom (b); projected DOS for a Ga1 atom (c) and projected DOS for a CO molecule (d). COOP curves for the Pd-Pd (e), Pd-Ga (f), Pd-C (g) and C-O (h) bonds before (red dashed line) and after (black full line) CO adsorption. (For interpretation of the color information in this figure legend, the reader is referred to the web version of the article.)

Please cite this article in press as: P. Bechthold, et al., CO adsorption on PdGa(1 0 0), (1 1 1) and $(\bar{1}\,\bar{1}\,\bar{1})$ surfaces: A DFT study, Appl. Surf. Sci. (2014), http://dx.doi.org/10.1016/j.apsusc.2014.01.074

Table 2
Electron orbital occupation, overlap population (OP), ΔOP% and distances for the PdGa low-index planes before and after CO adsorption.

Structure	Electronic occupation			Bond type	OP	ΔOP%	Distances (Å)
	s	p	d				
C-O (vacuum)							
C	0.44	0.38	0.00	C-O	0.854		1.143
O	1.61	3.56	0.00				
PdGa(1 0 0)							
Pd	0.74	0.54	9.77	Pd_1-Pd_2	0.053		3.063
				Pd_1-Pd_3	0.118		3.011
Ga	1.73	0.42	0.00	Pd_1-Ga_1	0.116		2.643
				Pd_1-Ga_2	0.124		2.607
CO/PdGa(1 0 0)							
Pd	0.57	0.76	9.70	Pd_1-Pd_2	0.028	−47.2	3.187
				Pd_1-Pd_3	0.088	−25.4	3.046
Ga	1.71	0.34	0.00	Pd_1-Ga_1	0.099	−14.6	2.618
				Pd_1-Ga_2	0.055	−54.6	2.835
C	1.12	4.44	0.00	Pd_1-C	0.887		1.961
O	1.62	5.86	0.00	C-O	0.426	−50.4	1.156
PdGa(1 1 1)							
Pd	0.91	0.24	9.83	Pd_i-Pd_{ii}	0.106		3.007
Ga	1.66	0.50	0.00	Pd_i-Ga_i	0.195		2.487
CO/PdGa(1 1 1)							
Pd	0.62	0.76	9.74	Pd_i-Pd_{ii}	0.062	−41.5	3.075
Ga	1.67	0.43	0.00	Pd_i-Ga_i	0.148	−21.1	2.580
C	1.11	4.47	0.00	Pd_i-C	0.912		1.976
O	1.62	5.86	0.00	C-O	0.419	−51.2	1.154
PdGa ($\bar{1}\,\bar{1}\,\bar{1}$)							
Pd	0.63	0.37	9.77	Pd_I-Pd_{II}	0.084		2.948
Ga	1.68	0.42	0.00	Pd_I-Ga_I	0.193		2.451
CO/PdGa ($\bar{1}\,\bar{1}\,\bar{1}$)							
Pd	0.55	0.77	9.67	Pd_I-Pd_{II}	0.052	−38.1	3.042
Ga	1.70	0.38	0.00	Pd_I-Ga_I	0.134	−30.6	2.565
C	1.11	4.48	0.00	Pd_I-C	0.887		1.976
O	1.62	5.86	0.00	C-O	0.417	−51.4	1.154

which is in agreement with our results for the (1 1 1) and ($\bar{1}\,\bar{1}\,\bar{1}$) surfaces. In the case of the (1 0 0) plane we found a 7.8° tilted configuration. From the analysis of IR data, Kovnir et al. [13] assigned an on top position for CO on the PdGa intermetallic compound.

As mentioned before, the PdGa intermetallic compound [22–24] has each Pd atom surrounded by seven Ga atoms. When the planes are generated from the bulk, an isolated Pd atom is exposed. Therefore, a comparison with the PdCO molecule and Pd_nCO ($n = 1$–9) is

Table 3
Orbital by orbital percentage contributions to Pd-Pd, Pd-Ga, Pd-C, and C-O overlap populations (%COOP) for Co/PdGa(1 0 0), (1 1 1) and ($\bar{1}\,\bar{1}\,\bar{1}$) system.

PdGa (1 0 0)		Pd_1-Pd_2		Pd_1-Ga_1	Pd_1-C		C-O[a]
		Clean	CO	Clean	CO	CO	
	s-s	14.4	6.8	9.6	12.6	19.2	25.7
	s-p	34.4	32.9	70.7	37.7	36.8	62.8
	s-d	6.3	8.3	0.0	0.0	0.6	–
	p-p	20.9	26.6	1.4	34.0	42.5	11.5
	p-d	24.0	25.4	18.3	15.7	0.9	0.0
	d-d	0.0	0.0	–	–	–	–
PdGa (1 1 1)		Pd_i-Pd_{ii}		Pd_i-Ga_i	Pd_i-C		C-O
		Clean	CO	Clean	CO	CO	
	s-s	32.1	11.9	9.7	16.8	19.8	26.0
	s-p	35.2	35.8	71.3	46.2	35.0	62.6
	s-d	4.5	10.7	0.4	1.0	0.9	–
	p-p	9.1	16.7	1.8	16.8	43.1	11.4
	p-d	19.1	24.9	16.8	19.2	1.2	–
	d-d	0.0	0.0	–	–	–	–
PdGa ($\bar{1}\,\bar{1}\,\bar{1}$)		Pd_I-Pd_{II}		Pd_I-Ga_I	Pd_I-C		C-O
		Clean	CO	Clean	CO	CO	
	s-s	13.8	7.8	13.0	24.0	20.7	25.8
	s-p	37.8	27.8	66.1	39.1	35.8	62.6
	s-d	8.9	12.2	0.0	0.0	0.8	–
	p-p	13.3	21.8	1.9	19.1	41.5	11.6
	p-d	26.2	30.4	19.0	17.8	1.2	–
	d-d	0.0	0.0	–	–	–	–

[a] The orbital by orbital percentage contributions for C-O bond in vacuum is s-p 100%.

Please cite this article in press as: P. Bechthold, et al., CO adsorption on PdGa(1 0 0), (1 1 1) and ($\bar{1}\,\bar{1}\,\bar{1}$) surfaces: A DFT study, Appl. Surf. Sci. (2014), http://dx.doi.org/10.1016/j.apsusc.2014.01.074

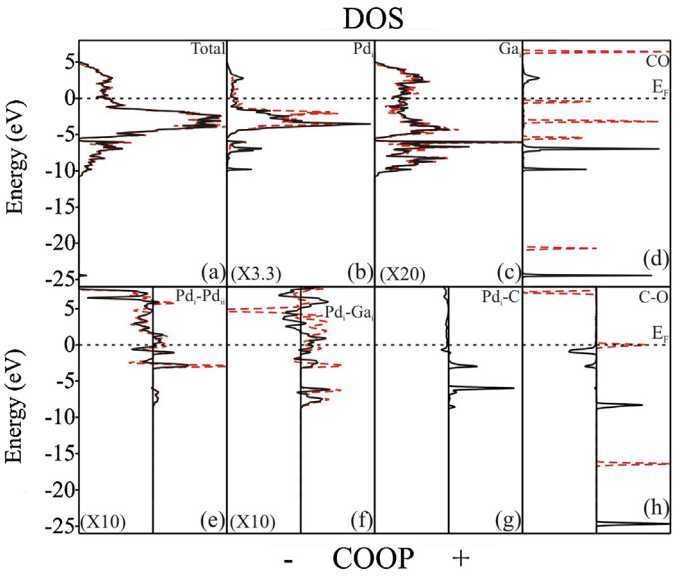

Fig. 4. Total DOS curves for the PdGa(1 1 1) surface (a); projected DOS for a Pd1 atom (b); projected DOS for a Ga1 atom (c) and projected DOS for a CO molecule (d). COOP curves for the Pd-Pd (e), Pd-Ga (f), Pd-C (g) and C-O (h) bonds before (red dashed line) and after (black full line) CO adsorption. (For interpretation of the color information in this figure legend, the reader is referred to the web version of the article.)

relevant. The gas phase experimental study of this molecule found a linear geometry with a $^1\Sigma^+$ ground state and Pd-C and C-O distances of 1.845 Å and 1.137 Å, respectively [50]. The computed Pd-C and C-O bond strengths, for all the surfaces under study, shows a noticeable degree of convergence of values reported in recent years [50]. DFT and all electron (CCSD(T)) calculations including relativistic effects are in agreement with experimental data [42,43]. In the case of Pd_nCO clusters, the DFT study by Bertin et al. [44] predicted a linear geometry if $n = 1$ with the CO bond length (1.18 Å) not appreciably modified after the interaction with a single Pd atom.

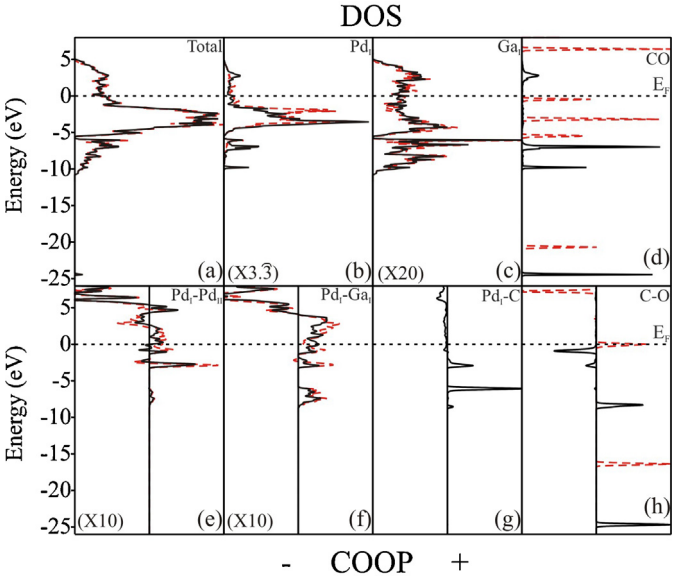

Fig. 5. Total DOS curves for the PdGa ($\bar{1}\bar{1}\bar{1}$) surface (a); projected DOS for a Pd1 atom (b); projected DOS for a Ga1 atom (c) and projected DOS for a CO molecule (d). COOP curves for the Pd-Pd (e), Pd-Ga (f), Pd-C (g) and C-O (h) bonds before (red dashed line) and after (black full line) CO adsorption. (For interpretation of the color information in this figure legend, the reader is referred to the web version of the article.)

Schultz et al. present similar results from *ab-initio* calculations for Pd_nCO ($n = 1,2$) [45]. Zanti and Peeters presented a DFT study of small Pd_n clusters ($n = 1$–9)-CO [46]. Their results ($d_{Pd\text{-}C} = 1.867$ and $d_{C\text{-}O} = 1.138$ Å) are close to our present calculations when n = 1. Kalita and Deca reported a Pd-CO distance and C-O bond length in neutral and charged Pd_1CO of 1.868 and 1.161 Å, respectively [47].

Considering the electronic structure, and as expected, we found no significant changes in the Fermi level after CO adsorption (see Figs. 3a, 4a and 5a, solid black line). The Total DOS is dominated by the many bulk-like and surface Pd and Ga atoms, so that the changes are subtle but visible in the Pd projected DOS. Only in the (1 0 0) plane, we can see a little peak about to −10 eV that is the product of the interaction with CO. The plots in Figs. 3b, 4b and 5b shows a decrease in the Pd d band density and a small shift of about 0.60 eV to lower energies. A similar behavior was computed for the DOS of Pd atoms bonded to CO on the (1 1 0) FCC bare surface [38]. In a theoretical study of CO adsorption on Pd(2 1 0) surface Lischka et al. [41] described the CO bonding to the metal surface in terms of the Blyholder model [51] and in the analysis of the resulting mixed orbitals [52,53] upon CO adsorption, the Pd-d band center is shifted down to 0.56 eV. XPS results obtained by Kovnir et al. [13] indicate no change in the electronic structure of the PdGa intermetallic surface upon CO adsorption. These conclusions are in agreement with our present results on the effect of CO on the electronic structure of PdGa (1 0 0), (1 1 1) and ($\bar{1}\bar{1}\bar{1}$) surfaces.

Almost no change in DOS is detected for Ga after CO adsorption in the case of the (1 1 1) and ($\bar{1}\bar{1}\bar{1}$) surfaces (see Figs. 4c and 5c). However, a small peak at −10 eV appears in the Ga projected DOS curves for the (1 0 0) surface, which is consistent with a CO peak mediated by interaction with Pd. This fact can explain the tilted configuration of CO (see Fig. 3c). Figs. 3a, 4a and 5a show the total DOS of the system with CO contribution. The bands at ∼−5 and ∼−10 eV corresponds to contributions from CO orbitals interacting with Pd orbitals, which becomes stabilized after adsorption. This is clearly shown in Figs. 3d, 4d and 5d were the CO/PdGa projected DOS (solid black line) is shifted to lower energies. The peak at ∼−24.8 eV in the total DOS, for all surfaces, corresponds mainly to CO orbitals that almost do not interact at all with the surface (see Figs. 3a, 4a and 5a). This picture is similar to that computed by Lischka et al. [41]. It should be mentioned that projected DOS of CO shows very narrow bands for all the surfaces, which is an indication of an interaction with an "isolated Pd site".

An analysis of the bonding between CO and the surface reveals that the main contribution to the Pd-CO bond comes from s-p (between 35 and 37%), s-s (between 19 and 21%) and p-p (between 41 and 43%) orbitals. Less than 1.5% of the bonding comes from p-d interactions for all the surfaces considered (see Table 3). The Pd-CO bond is achieved at the expense of the Pd-Pd nearest neighbor (see Table 2 and Figs. 3e, 4e and 5e). Thus, the Pd-Pd bond overlap population (OP) involving Pd atoms directly bonded to CO is reduced to 47.2, 41.5 and 38.1% of its original values on the clean PdGa(1 0 0), (1 1 1) and ($\bar{1}\bar{1}\bar{1}$) surfaces, respectively. The COOP curves in Figs. 3e, 4e and 5e also show less bonding after CO adsorption. Paz-Borbon et al. [39] found an overall inflation of the Pd nano-clusters and a weakening of the metal-metal bonds when CO is adsorbed. The Pd-Ga OP also decreases when the CO is adsorbed (see Table 2 and Figs. 3f, 4f and 5f). We do not detect any direct Ga-CO bond interaction. Thus, the reason for this decrease could be the bonding to a Pd atom that interacts directly with the CO. Also when adsorbed, the CO move the Pd atom outwards the surface. Föttinger found that the detrimental effect in the metallic bonding is evidenced in the CO adsorption spectra. The driving force for the degradation by CO is likely the strong interaction of Pd with CO "pulling" the Pd to the surface [48].

Please cite this article in press as: P. Bechthold, et al., CO adsorption on PdGa(1 0 0), (1 1 1) and ($\bar{1}\bar{1}\bar{1}$) surfaces: A DFT study, Appl. Surf. Sci. (2014), http://dx.doi.org/10.1016/j.apsusc.2014.01.074

Regarding the C-O bond, its length is increased 1.3% after adsorption. The C-O bond is weakened due to 5σ donation and $2\pi^*$ back donation to the surface. This is shown in Table 2 where C 2p orbitals are more populated after CO adsorption being the p_x and p_y orbitals the more affected in all cases. The C-O OP decreases about 50% while its bond length change less than 1.3%. The Pd d orbital population changes between $0.26e^-$ and $0.33e^-$ for the surfaces considered, which is consistent with the main role of s-s and s-p interactions (see Table 3). The reasons for this C-O bond weakening are already discussed by Shultz et al. [45], Bertin et al. [44], Filatov et al. [42] and Zanti and Peeters [46]. According to the last authors, the intensity of back bonding results in the relocalization of 0.30e- from the 4d orbitals of Pd [46] and this is in agreement with our results.

4. Conclusion

The adsorption of CO in different surfaces of the $P2_13$ PdGa intermetallic compound has been studied by DFT calculation. The adsorption energies are −1.42, −1.36 and −1.59 eV with respect to the gas phase CO molecule for PdGa(1 0 0), (1 1 1) and ($\bar{1}\,\bar{1}\,\bar{1}$) surfaces. This result is similar to those computed for CO on top sites on FCC Pd metallic surfaces and Pd nano-clusters. The CO distance does not change significantly with respect to the isolated molecule but its overlap population decreases about 50% while a Pd-C bond is developed in all surfaces.

Our computed results are compatible with those from TDS spectrum that shows a dominant peak at ≈210 K for PdGa ($\bar{1}\bar{1}\bar{1}$). This desorption peak was attributed to CO bonded to the only Pd atom/cell in the surface layer.

The CO adsorbs atop on a Pd atom with a small tilt of 7.8° in the plane (1 0 0). There is also an analogy with the PdCO molecule and Pd_nCO (n = 1,9) clusters. In the case of (1 1 1) and ($\bar{1}\,\bar{1}\,\bar{1}$) surfaces, the CO is adsorbed in a top site perpendicular to the surface.

The Pd-CO bond is formed at the expenses of Pd-Pd (from a three center bond Pd-Ga-Pa) and Pd-Ga bonds. No direct interaction of CO with Ga is detected. The main contribution to Pd-CO bonding energy corresponds to s-s and s-p orbitals with less participation of Pd 4d orbitals. A back donation of about $0.26e^-$, $0.30e^-$ and $0.33e^-$ for PdGa(1 0 0), (1 1 1) and ($\bar{1}\,\bar{1}\,\bar{1}$) surfaces respectively is also computed.

The projected DOS of Pd shows a small shift to lower energies after CO adsorption (0.60 eV). The computed vibrational frequencies for the C-O adsorbed presents a red shift – compared with the gas phase CO – that is in agreement with experimental data reported in [13].

Acknowledgements

Our work was supported by ANPCyT through PICT 1770, and PIP-CONICET No. 114-200901-00272 and No. 114-200901-00068. research grants, as well as by SGCyT-UNS. E.A. Gonzalez, and P.V. Jasen and J.S. Ardenghi, and A. Juan are members of CONICET. P. Bechthold is a fellow researcher at this Institution.

References

[1] K. Kovnir, M. Armbrüster, D. Teschner, T.V. Venkov, F.C. Jentoft, A. Knop-Gericke, Y. Grin, R. Schlögl, A new approach to well-defined, stable and site-isolated catalysts, Sci. Technol. Adv. Mater. 8 (5) (2007) 420–427.
[2] A. Haghofer, K. Föttinger, F. Girgsdies, D. Teschner, A. Knop-Gericke, R. Schlögl, G. Rupprechter, In situ study of the formation and stability of supported Pd_2Ga methanol steam reforming catalysts, J. Catal. 286 (2012) 13–21.
[3] N. Iwasa, T. Mayanagi, N. Ogawa, K. Sakata, N. Takezawa, New catalytic functions of Pd–Zn, Pd–Ga, Pd–In, Pt–Zn, Pt–Ga and Pt–In alloys in the conversions of methanol, Catal. Lett. 54 (3) (1998) 119–123.
[4] D.R. Palo, R.A. Dagle, J.D. Holladay, Methanol steam reforming for hydrogen production, Chem. Rev. 107 (10) (2007) 3992–4021.
[5] N. Iwasa, T. Mayanagi, W. Nomura, M. Arai, N. Takezawa, Effect of Zn addition to supported Pd catalysts in the steam reforming of methanol, Appl. Catal. A 248 (1–2) (2003) 153–160.
[6] N. Iwasa, N. Takezawa, New supported Pd and Pt alloy catalysts for steam reforming and dehydrogenation of methanol, Top. Catal. 22 (2003) 215–224.
[7] S. Penner, H. Lorenz, W. Jochum, M. Stöger-Pollach, D. Wang, C. Rameshan, B. Klötzer, Pd/Ga2O3 methanol steam reforming catalysts: Part: I. Morphology, composition and structural aspects, Appl. Catal. A 358 (2009) 193–202.
[8] H. Lorenz, S. Penner, W. Jochum, C. Rameshan, B. Klötzer, Pd/Ga_2O_3 methanol steam reforming catalysts: Part: II. Catalytic selectivity, Appl. Catal. A 358 (2009) 203–210.
[9] C. Rameshan, W. Stadlmayr, S. Penner, H. Lorenz, L. Mayr, M. Hävecker, R. Blume, T. Rocha, D. Teschner, A. Knop-Gericke, R. Schlögl, D. Zemlyanov, N. Memmela, B. Klötzer, In situ XPS study of methanol reforming on PdGa near-surface intermetallic phases, J. Catal. 290 (2012) 126–137.
[10] M. Krajčí, J. Hafner, Structure and chemical reactivity of the polar three-fold surfaces of GaPd: A density-functional study, J. Chem. Phys. 138 (2013) 124703 (20).
[11] D. Rosenthal, R. Widmer, R. Wagner, P. Gille, M. Armbrüster, Y. Grin, R. Schlögl, O. Gröning, Surface Investigation of Intermetallic PdGa ($\bar{1}\bar{1}\bar{1}$), Langmuir 28 (2012) 6848–6856.
[12] J.C.H. Spence, J.M. Zuo, M. Okeeffe, K. Marthinsen, R. Hoier, On the minimum number of beams needed to distinguish enantiomorphs in X-ray and electron diffraction, Acta Crystallogr. Sect. A 50 (1994) 647–650.
[13] K. Kovnir, M. Armbrüster, D. Teschner, T.V. Venkov, L. Szentmiklosi, F.C. Jentoft, A. Knop-Gericke, Y. Grin, R. Schlögl, In situ surface characterization of the intermetallic compound Pd-Ga–A highly selective hydrogenation catalyst, Surf. Sci. 603 (10–12) (2009) 1784–1792.
[14] M. Armbrüster, K. Kovnir, D. Teschner, M. Behrens, Y. Grin, R. Schlögl, Pd–Ga intermetallic compounds as highly selective semihydrogenation catalysts, J. Am. Chem. Soc. 132 (2010) 14745–14747.
[15] A. Ota, M. Armbrüster, M. Behrens, D. Rosenthal, M. Friedrich, I. Kasatkin, F. Girgsdies, W. Zhang, R. Wagner, R. Schlögl, Intermetallic compound Pd_2Ga as a selective catalyst for the semi-hydrogenation of acetylene: from model to high performance systems, J. Phys. Chem. C 115 (2011) 1368–1374.
[16] M. Klanjšek, A. Gradišek, A. Kocjan, M. Bobnar, P. Jegli, M. Wencka, Z. Jaglicic, P. Popcevic, J. Ivkov, A. Smontara, P. Gille, M. Armbrüster, Y. Grin, J. Dolinšek, PdGa intermetallic hydrogenation catalyst: an NMR and physical property study, J. Phys.: Condens. Matter. 24 (2012) 085703, 9 pp.
[17] S.E. Collins, M.A. Baltanas, A.L. Bonivardi, Mechanism of the decomposition of adsorbed methanol over a $Pd/\alpha,\beta\text{-}Ga_2O_3$ catalyst, App. Catal. A: Gen. 295 (2) (2005) 126–133.
[18] J. Prinz, R. Gaspari, C.A. Pignedoli, J. Vogt, P. Gille, M. Armbrüster, H. Brune, O. Gröning, D. Passerone, R. Widmer, Isolated Pd sites on the intermetallic PdGa(1 1 1) and PdGa ($\bar{1}\bar{1}\bar{1}$) model catalyst surfaces, Angew. Chem. Int. Ed. 51 (2012) 9339–9343.
[19] T. Skála, D. Baca, J. Libra, N. Tsud, V. Nehasil, S. Nemšák, K.C. Prince, V. Matolín, A photoemission study of carbon monoxide interaction with the Ga–Pd(1 1 0) system, Thin Solid Films 517 (2) (2008) 773–778.
[20] P. Bechthold, P. Jasen, E. González, A. Juan, Hydrogen Adsorption on PdGa(1 1 0): A DFT Study, J. Phys. Chem. C 116 (2012) 17518–17524.
[21] P. Bechthold, P. Jasen, J. Ardenghi, E. González, A. Juan, Ab initio study of CO adsorption on PdGa(1 1 0), Comp. Mater. Sci. 71 (2013) 192–196.
[22] E. Hellner, F. Laves, Z.A. Naturforsch, In und Ga in Legierungen mit einigen Übergangselementen (Ni, Pd, Pt, Cu, Ag und Au), Kristallchemie des. 2 (1947) 177–183.
[23] M.K. Bhargava, A.A. Gadalla, K. Schubert, Koexistente phasen vom FeSi-Typ in den mischungen Ni-Pd-Ga und Ni-Pt-Ga, J. Less-Comm. Met. 42 (1975) 69–76.
[24] G. Phragmen, Om järn-kisellegeringarnas byggnad, Jernkontor. Ann. 107 (1923) 121.
[25] M. Armbrüster, H. Borrmann, M. Wedel, Y. Prots, R. Giedigkeit, P. Gille, Z. Kristallogr, Refinement of the crystal structure of palladium gallium (1:1), PdGa, NCS 225 (2010) 617–618.
[26] G. Kresse, J. Hafner, Ab initio molecular dynamics for liquid metals, Phys. Rev. B 47 (1993) 558–561.
[27] G. Kresse, J. Furthmüller, Efficient iterative schemes for ab initio total-energy calculations using a plane-wave basis set, Phys. Rev. B 54 (1996) 11169–11186.
[28] G. Kresse, J. Furthmüller, Efficiency of ab-initio total energy calculations for metals and semiconductors using a plane-wave basis set, Comput. Mater. Sci. 6 (1996) 15–50.
[29] D. Vanderbilt, Soft self-consistent pseudopotentials in a generalized eigenvalue formalism, Phys. Rev. B 41 (1990) 7892–7895.
[30] B. Hammer, L.B. Hansen, J.K. Nørskov, Improved adsorption energetics within density-functional theory using revised Perdew-Burke-Ernzerhof functionals, Phys. Rev. B 59 (1999) 7413–7421.
[31] H.J. Monkhorst, J.D. Pack, 13 Special points for Brillouin-zone integrations, Phys. Rev. B (1976) 5188–5192.
[32] R.F.W. Bader, Atoms in Molecules - A Quantum Theory, Oxford University, Oxford, 1990.
[33] G. Glockler, Carbon–oxygen bond energies and bond distances, J. Phys. Chem. 62 (9) (1958) 1049–1054.
[34] R. Hoffmann, Solid & Surface: A Chemist's View of Bonding in Extended Structures, first ed., Wiley-VCH, New York, 1989.

Please cite this article in press as: P. Bechthold, et al., CO adsorption on PdGa(1 0 0), (1 1 1) and ($\bar{1}\,\bar{1}\,\bar{1}$) surfaces: A DFT study, Appl. Surf. Sci. (2014), http://dx.doi.org/10.1016/j.apsusc.2014.01.074

[35] P. Ordejón, E. Artacho, J.M. Soler, Self-consistent order-N density-functional calculations for very large systems, Phys. Rev. B 53 (1996) R10441–R10444.
[36] J.M. Soler, E. Artacho, J.D. Gale, A. Garcia, J. Junquera, P. Ordejón, D. Sanchez-Portal, The SIESTA method for ab initio order-N materials simulation, J. Phys. Condes. Matter 14 (2002) 2745–2779.
[37] R. Chen, Z. Chen, B. Ma, X. Hao, N. Kapur, J. Hyun, K. Cho, B. Shan, CO adsorption on Pt (1 1 1) and Pd (1 1 1) surfaces: A first-principles based lattice gas Monte-Carlo study, Comput. Theor. Chem. 987 (2012) 77–83.
[38] S. Pick, Density-functional study of the CO chemisorption on bimetallic Pd-Sn(1 1 0) surfaces, Surf. Sci. 603 (16) (2009) 2652–2657.
[39] L.O. Paz-Borbon, R.L. Johnston, G. Barcaro, A. Fortunelli, Chemisorption of CO and H on Pd, Pt and Au nanoclusters: a DFT approach, Eur. Phys. J. D 52 (2009) 131–134.
[40] G. Herzberg, K.P. Huber, Molecular Spectra and Molecular Structure IV, Van Nostrand Reinhold Company, New York, 1979.
[41] M. Lischka, C. Mosch, A. Groß, CO and hydrogen adsorption on Pd(210), Surf. Sci. 570 (2004) 227–236.
[42] M. Filatov, On the binding of carbonyl to a single palladium atom, Chem. Phys. Lett. 373 (2003) 131–135.
[43] Z.J. Wu, H.L. Li, H.J. Zhang, Electronic structures of MCO (M = Nb, Ta, Rh, Ir, Pd, Pt) molecules by density functional theory, J. Meng J. Phys. Chem. A 108 (2004) 10906–10910.
[44] V. Bertin, E. Agacino, R. López-Rendon, E. Poulain, The CO chemisorption on some active sites of Pd clusters: A DFT study, J. Mol. Struct.: Teochem. 769 (2006) 243–248.
[45] N.Z. Schultz, B.F. Gherman, C.J. Cramer, D.G. Trohlar, Pd_nCO (n = 1,2): accurate ab initio bond energies, geometries, and dipole moments and the applicability of density functional theory for fuel cell modeling, J. Phys. Chem. B 110 (2006) 24030–24046.
[46] G. Zanti, D. Peeters, DFT study of small palladium clusters Pd_n and their interaction with a CO ligand (n = 1–9), Eur. J. Inorg. Chem. 26 (2009) 3904–3911.
[47] B. Kalita, R.C. Deka, DFT study of CO adsorption on neutral and charged Pd_n(n = 1–7) clusters, Eur. Phys. J. D 53 (2009) 51–58.
[48] K. Föttinger, The effect of CO on intermetallic PdZn/ZnO and Pd_2Ga/Ga_2O_3 methanol steam reforming catalysts: A comparative study, Catal. Today 208 (2013) 106–112.
[49] Y. Grin, F.R. Wagner, M. Armbruster, M. Kohouta, A. Leithe-Jasper, U. Schwarz, U. Wedig, H.G. von Schnering, $CuAl_2$ revisited: composition, crystal structure, chemical bonding, compressibility and Raman spectroscopy, J. Solid State Chem. 179 (2006) 1707–1719.
[50] N.R.J. Walker, K.-H. Hui, C.L. Gerry, Microwave spectrum, geometry, and hyperfine constants of PdCO, J. Phys. Chem. A 106 (2002) 5803–5808.
[51] G. Blyholder, Molecular orbital view of chemisorbed carbon monoxide, J. Phys. Chem. 68 (1964) 2772–2777.
[52] A. Föhlisch, M. Nyberg, P. Bennich, L. Triguero, J. Hasselström, O. Karis, L.G.M. Pettersson, A. Nilsson, The bonding of CO to metal surfaces, J. Chem. Phys. 112 (4) (2000) 1946–1959.
[53] A. Föhlisch, M. Nyberg, J. Hasselström, O. Karis, L.G.M. Pettersson, A. Nilsson, How carbon monoxide adsorbs in different sites, Phys. Rev. Lett. 85 (2000) 3309–3312.

Please cite this article in press as: P. Bechthold, et al., CO adsorption on PdGa(1 0 0), (1 1 1) and ($\bar{1}\,\bar{1}\,\bar{1}$) surfaces: A DFT study, Appl. Surf. Sci. (2014), http://dx.doi.org/10.1016/j.apsusc.2014.01.074